Solid Particle Erosion Resistance of Protective Ion-Plasma Coating Formed on Full-Scale Objects Based on Modern Additive Technologies

A.B. Tkhabisimov, A.F. Mednikov, M.R. Dasaev, G.V. Kachalin, O.S. Zilova

Abstract*: *This paper presents the results of the research concerning solid particle erosion resistance of protective ion-plasma coating formed on experimental samples and compressor rotating blades of an energy gas turbine installation (full-scale objects). The coating was made using selective laser melting of titanium powder based on Ti-6Al-4V. The main characteristics (composition, hardness, structure) of the obtained titanium alloy, as well as of the considered chromium carbide-based coating (composition, hardness, structure, thickness) are considered. The work also presents a comparison of the results of solid particle erosion tests on experimental samples and material of coated and uncoated blades carried out under conditions close to real operating conditions. It has been established that the application of the proposed coating on the obtained full-scale object allows for at least two times longer duration of the incubation-transition period and reduces the steady-state rate of solid particle erosion. The obtained effect extends both to the concave and convex sides of the test blade with a specific difference their wear during metallographic studies.

Index Terms*: *additive technologies, blades, compressor, experimental test, metallography, protective coating, samples, solid particle erosion.

I. INTRODUCTION

Nowadays, additive technologies allow using a wide range of different materials, such as engineering plastics, composite powders, metals and alloys, ceramics and sand. 3D printing is used in the aerospace and automotive industries, electronics and medicine, science and education, as well as many other spheres of human activity [1]-[7]. The emergence of these technologies and the increase in the diversity of materials used make it possible to expand their application from objects prototyping to replacing traditional manufacturing technologies.

Unlike traditional technologies, with the loss of consumables up to 80% or more, additive technologies are much more efficient, as the equipment software allows one to accurately calculate the number of consumed materials. For example, casting or stamping does not allow manufacturing products that are complex in terms of geometry. Therefore, the parts for cooling systems with a mesh design cannot be produced by traditional methods [8]. In turn, the existing industrial 3D printers allow printing products of almost any complexity [9]-[11]. However, when used to print a complex-profile blade unit, the problems arise related to the ability of the printed material to withstand the various types of wear, to which it is exposed during operation, and the ways to protect it [12].

In this work, we solve the problem of increasing the resistance to solid particle erosion of titanium rotating blades of the first stages of gas turbine installation compressors made using additive technologies and susceptible to wear by solid particles coming along with the flow of outside air. One of the possible ways of passive protection of the blades' material is the formation of a wear-resistant ion-plasma coating with specific characteristics [13]-[17]. This method has been proposed and studied in this work.

II. PRODUCTION OF EXPERIMENTAL SAMPLES AND COMPRESSOR ROTATING BLADES USING ADDITIVE TECHNOLOGIES

To produce experimental samples and rotating blades of a compressor stage, an industrial 3D printer Concept Laser M2 Cusing Multilaser was used [18]. The printer implements the selective laser melting method of reactive and non-reactive metal powders due to the impact of two asynchronous ytterbium fiber lasers with great power [4], [19]-[20]. The use of this method can significantly reduce the production costs and time typical for traditional methods of casting and stamping [2]. Such printers are widely used in aviation, engineering and energetics to produce engine components, gas turbines, fuel systems, etc. [3]. During the printing process (Fig. 1), the powder (from metals or alloys) is completely melted, resulting in a homogeneous mass.

Revised Manuscript Received on May 06, 2019

A.B. Tkhabisimov, National Research University "MPEI", Moscow, Russia.
A.F. Mednikov, National Research University "MPEI", Moscow, Russia.
M.R. Dasaev, National Research University "MPEI", Moscow, Russia.
G.V. Kachalin, National Research University "MPEI", Moscow, Russia.
O.S. Zilova, National Research University "MPEI", Moscow, Russia

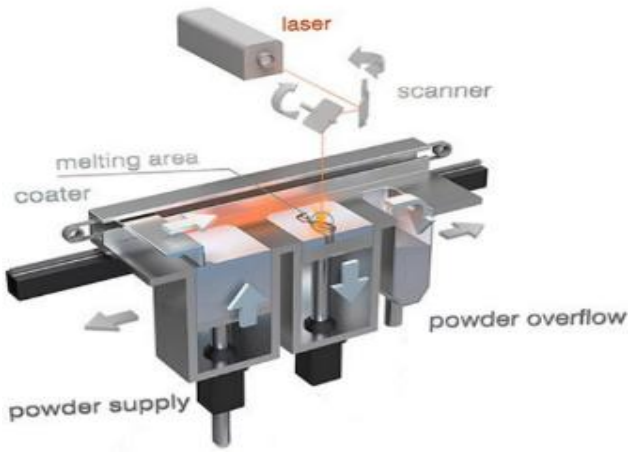

Fig. 1. The scheme of operation of the 3D printer Concept Laser M2 Cusing Multilaser [18]

To form a coating and run solid particle erosion tests, experimental samples were produced in the shape of disks (Fig. 2a) [21]. The scaled parts of the rotating blades of one of the first stages of the power gas turbine installation were also made to confirm the characteristics of the studied coating during its formation on full-scale objects (Fig. 2b).

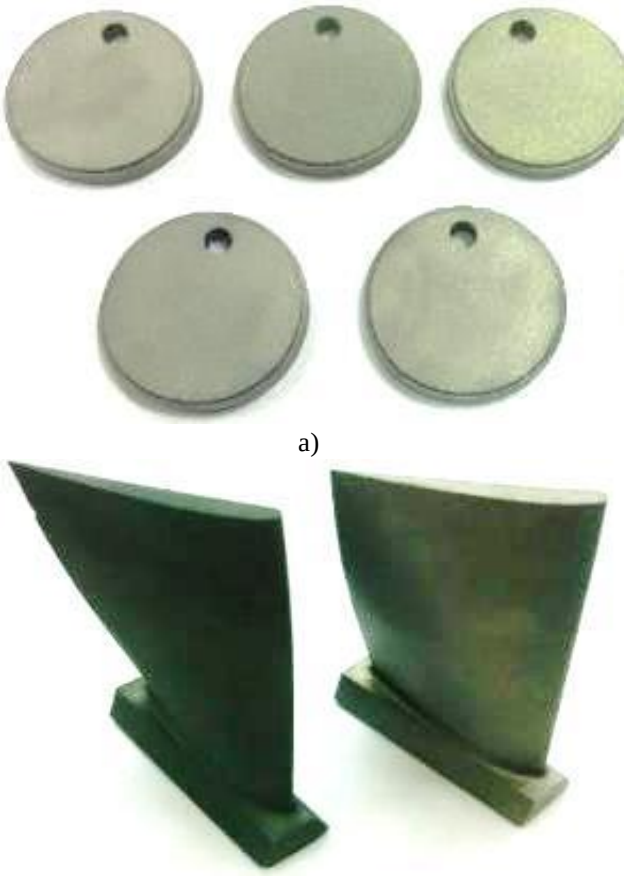

a)

b)

Fig. 2. Experimental samples (a) and rotating blades of the compressor stage (b) made using additive technologies

The chemical composition of the powder used to produce experimental samples and parts of the compressor blades is presented in Table I.

Table I. The chemical composition of titanium powder Ti-6Al-4V

Element	Mass, %
Ti	88÷90
Al	5.5÷6.5
V	3.5÷4.5
Fe	< 0.25
O	< 0.08
C	< 0.08
N	< 0.05
H	< 0.012

III. FORMATION OF ION-PLASMA COATING

To form an ion-plasma coating, a pilot installation "Gefest+" National Research University "MPEI" (Fig. 3) was used. The installation includes the following main components: vacuum chamber; mechanism for moving samples (products) inside the vacuum chamber; high vacuum pumping system; water supply and compressed air supply systems; process gas supply and distribution system; technological sources for the formation of coating with power supplies.

Fig. 3. The "Gefest+" NRU "MPEI" installation

The installation is equipped with four unbalanced planar magnetrons with coaxial input. It is designed to produce a coating on the surface of products of different metals and alloys due to ionic sputtering of the magnetron target in a plasma-forming inert gas.

Magnetrons with chromium cathode targets were used to synthesize a coating based on chromium carbide (Cr-CrC). To obtain the compounds from chromium carbide, methane of high purity was dosed into the chamber. Fig. 4 shows the experimental samples and part of the compressor blade in the vacuum chamber of the "Gefest+" after the coating formation process.

a) b)

Fig. 4. Part of the compressor blade (a) and the experimental samples (b), mounted on the technological equipment of the vacuum chamber of the "Gefest+" installation

IV. METHODS AND EQUIPMENT FOR METALLOGRAPHIC RESEARCH

The following analytical equipment was used to conduct research and control of the characteristics of the coating formed on the experimental samples ("witness samples") and on parts of the compressor rotating blades, which are a part of the unique research installation "Hydraulic impact test facility "Erosion-M" of the NRU "MPEI" [22]:

- Posi Tector coating thickness gauge for measuring coating thickness;
- Surftest SJ-210 portable contact profilometer for determining the surface roughness of the samples and objects before and after coating formation;
- hardness tester for low loads DuraScan 20 and microhardness tester MHT-10 for determining the value of microhardness of the formed coating;
- laboratory image analysis complex for an optical microscope Axiovert 25CA;
- laboratory complex Calotest for determining the thickness of the coating and the production of ball section;
- a system of elemental analysis of coating based on a glow discharge spectrometer and an electronic scanning emission microscope TESCAN MIRA 3 LMU for the study of the composition and structure of the coating. Images of thin sections were obtained in the mode of back-scattered electrons, giving a contrast atomic number. The study of the surface morphology was also carried out using an electronic microscope, in the mode of secondary electrons, which provides information about the surface topography.

The analysis of the coatings by electron spectroscopy was carried out both on the surface and transverse sections. To produce cross-sections, a set of equipment for sample preparation was used, which included a semi-automatic grinding and polishing machine BETA/1, a cutting-off automatic table power machine PowerMet 3000 and an electro-hydraulic press for pressing samples into resins SIMPLIMET 1000.

For the original uncoated samples, produced with similar additive technology, the chemical composition of the sample material was monitored by a system for spectral analysis of the alloys. The microhardness of the printed material was determined.

V. SOLID PARTICLE EROSION TEST METHOD

The tests were carried out on the experimental stand of NRU "MPEI", designed for comprehensive research of the solid particle erosion processes of structural materials, protective coatings and various methods of hardening in accordance with ASTM G76-13 [23]. This stand is a jet-type installation and allows testing at varying costs, air-abrasive flow angles of attack and sample surface temperatures. The technique and instrumentation of the stand allow for the use of various criteria for assessing the intensity of the solid particle erosion process, including in a dimensionless form. The stand is shown in Fig. 5.

Fig. 5. The experimental stand

As a carrier medium, the stand uses air purified from impurities and moisture. The temperature of the stream is constant, and the temperature of the sample can vary from ambient temperature to 600ºC. Al_2O_3 (electrocorundum) particles are used as the abrasive material.

During the tests, the air-abrasive jet was directed at the flat surface of the sample, the angle of which was adjusted with respect to the jet using a special fastening. The exposure time of the samples ranged from 5 to 60 minutes, the speed of the air-abrasive flow was 170 m/s, the consumption of solid abrasive particles – 6·10-5 kg/s, the surface temperature of the samples – 25ºC.

To study the influence of the location of the concave and convex sides (relative to the air-abrasive flow) on the wear rate, a special holder was made using additive technologies (Fig. 6).

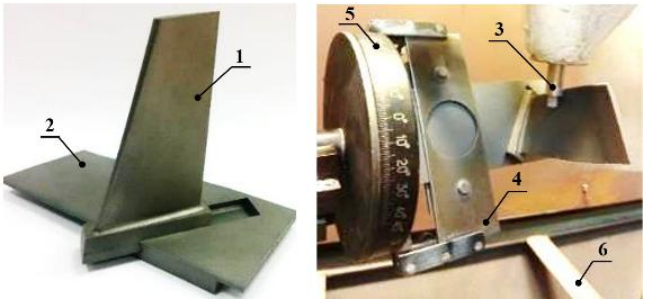

a) b)

1 – part of the compressor blade; 2 – holder;
3 – stabilizing tube; 4 – clamping plate;
5 – rotating part of the mount; 6 – stand's camera

Fig. 6. Fastening part of the blade in the holder (a) and the location of the blade in the chamber of the stand (b) relative to the nozzle when conducting the research

The structure design combines the holder and the special fastening and makes it possible to organize the direction of the air-abrasive flow at an average angle of maximum wear of plastic materials 30º (which also include titanium [11]) to the surface of the swirling blade. The concept of "average angle" is introduced as a certain assumption adopted during the conduct of these studies. Because the blade has a profile twist in height that is necessary to optimize the flow of the working fluid and minimize aerodynamic losses, it was assumed that the surface of both the concave and convex sides of the blades was close to flat.

The mass loss of the object was calculated by the formula:

$$\Delta m_i = m_o - m_i$$

where m_o – the initial mass of the object of experimental research; m_i – the mass of the object after the experiment; i – the number of the experiment.

As a result of the study of a series of coated samples, the kinetic curves of abrasive wear $\Delta m = f(t)$ were obtained (Fig. 7). A comparative analysis of the main characteristics of the abrasive wear process was carried out considering the incubation-transition period (t_{IT}) duration and the steady-state speed solid particle erosion ($E_{SSS} = tg\alpha$).

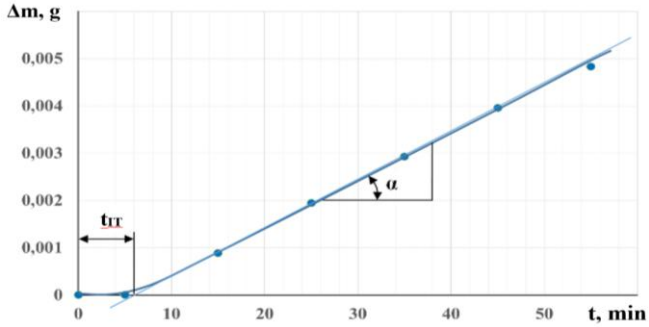

Fig. 7. Curve of solid particle erosion of plastic material

VI. RESULTS

The results of measuring the thickness, microhardness and composition of the coatings, as well as surface roughness, are presented in Table II.

Table II. The results of measuring the microhardness, thickness and composition of the coating

№	Sample description	Coating composition	Coating thickness δ, μm	Microhardness HV 0.05	Ra, μm	Rz, μm
1	Disk from Ti-6Al-4V without coating	-	-	420±40	4.2±0.6	30±3
2	Blade from Ti-6Al-4V without coating	-	-	430±70	9.8±1.3	68±8
3	Disk from Ti-6Al-4V with Cr-CrC coating	96% Cr, 2% C, 1% Ti, 1% O	8.7±0.6	1620±90	3.3±0.3	31±8
4	Blade from Ti-6Al-4V with Cr-CrC coating	95.5% Cr, 3% C, 1.5 % Ti	8.1±0.6	1270±90	3.1±1.3	21±5

The control of coating characteristics on the blades showed the following results: the Cr-CrC coating is uniformly formed over the entire working surface of the blade (Fig. 8) and has a multi-layer structure with a total thickness of 7-9 microns (Fig. 9). The average microhardness of the coating on the working surfaces reaches 1270÷1620 HV 0.05. The microhardness of uncoated samples averages 420÷430 HV 0.05.

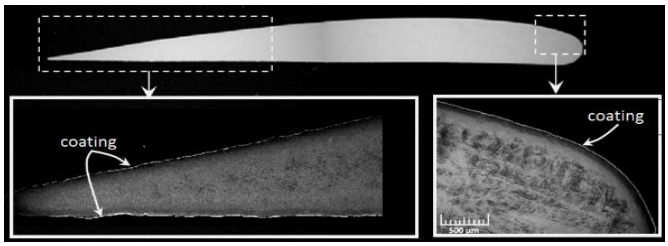

Fig. 8. Cross-section of the rotating blade of the compressor from titanium alloy

Ti6Al4V with the coating based on Cr-CrC

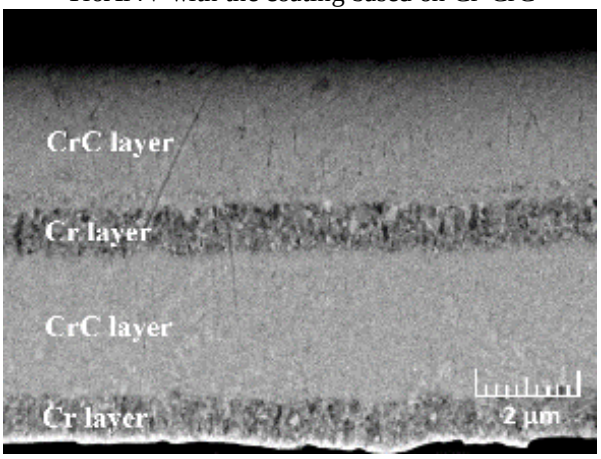

a)

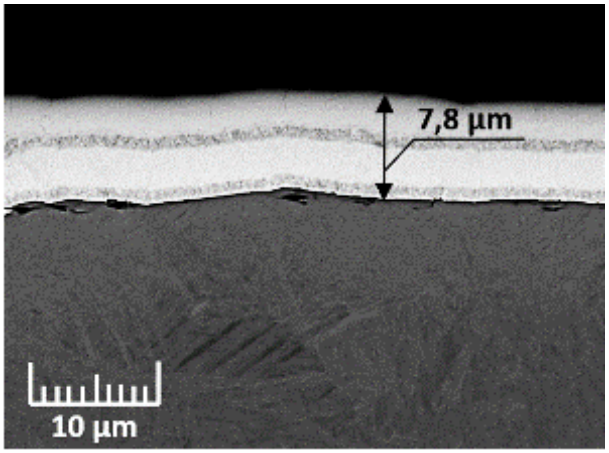

b)

Fig. 9. The image of the transverse section of the rotating blade with the coating (a) and the results of measuring the thickness of the Cr-CrC coating (b)

Fig. 10 shows the change in the elemental composition over the depth of the surface layer. Elemental analysis showed that the main element of the coating is chromium (80-85%), as well as carbon (12-15%) and various impurities.

The surface structure of the coating is granular. The grain size varies in the range from 30 to 240 nm (Fig. 11).

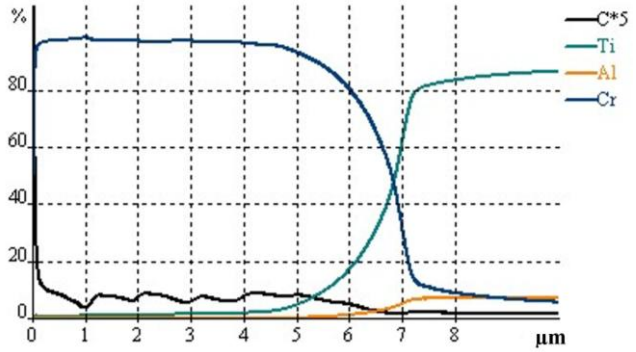

Fig. 10. Changes in the elemental composition over the depth of the surface layer of the Ti6Al4V titanium alloy with Cr-CrC coating

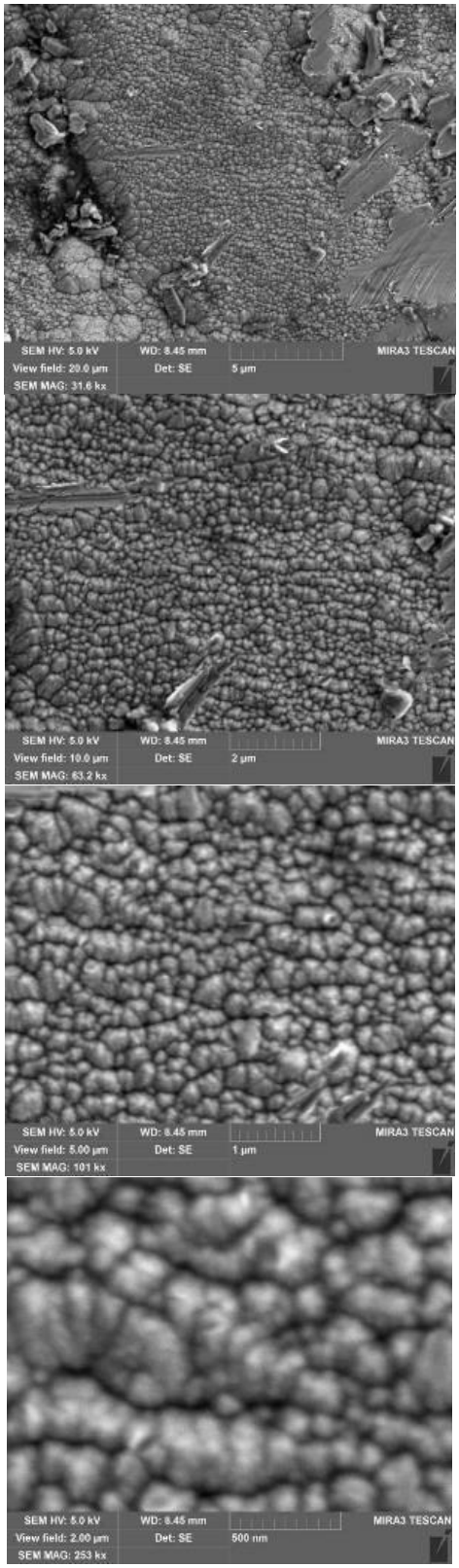

Fig. 11. Surface morphology of Cr-CrC coating

Interest

During the studies, experimental dependences of the sample mass loss Δm (g) on the exposure time on the stand t (min) were obtained, reflecting the kinetics of the solid particle erosion process of the material on the concave (Fig. 12) and convex (Fig. 13) sides from Ti-6Al-4V titanium alloy with Cr-CrC coating.

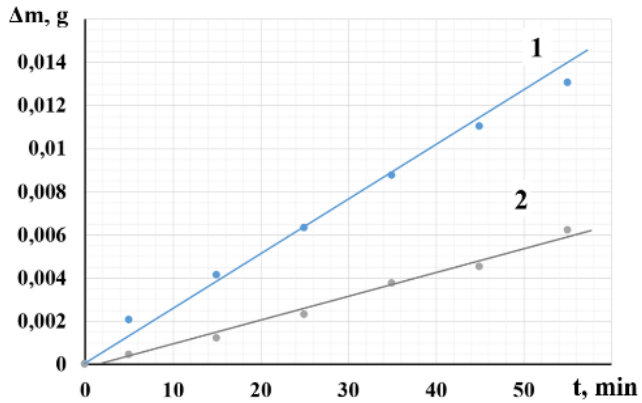

Fig. 12. Results of solid particle erosion tests of compressor blades without coating (1) and with a coating (2) (the tests on the concave side)

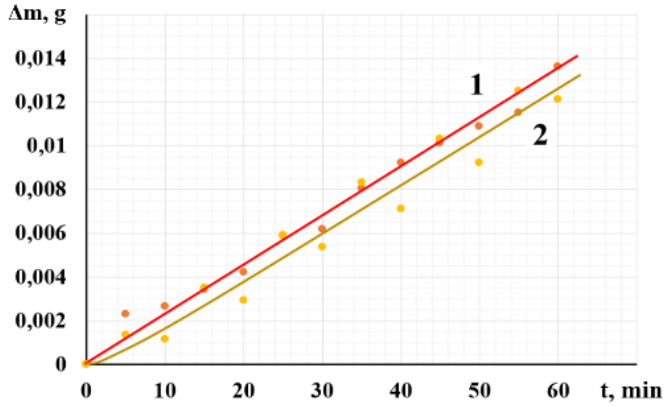

Fig. 13. Results of solid particle erosion tests of compressor blades without the coating (1) and with the coating (2) (the tests on the convex side)

Based on the constructed dependencies, the numerical indicators of the main characteristics of the solid particle erosion process, such as the duration of the incubation transition period and the steady-state wear rate were determined (Table III).

Table III. Numerical results of studies of the process of solid particle erosion of compressor blades with and without the protective coating

Side of the compressor blade	**Uncoated/Coated**	
	The duration of the incubation-transition period, min	The steady wear rate of 10^{-9}, kg/s
Concave side	0.5/1.5	4/2
Convex side	0.5/1	3.8/3.8

VII. RESULTS ANALYSIS

The surface roughness of samples from Ti-6Al-4V with the coating is from 3.1 to 3.3 μm, considering that the initial surface is from 4.2 to 9.8 μm. The high roughness of the produced compressor blade can be explained by the insufficient quality of the finishing treatment of the printed product surfaces.

The blades with and without the coating after the experimental studies are presented in Table IV. The table clearly shows that there is a definite difference between the geometry of the "abrasive" traces. On the concave side, the trace is more elongated, but on the convex side, the trace is wider. Most likely, this is due to the fact that the real area of interaction of the air-abrasive flow with the concave side of the blade is more than with the convex one.

Additionally, Table IV presents photographs of the morphology of the surfaces of the blades in the area of the "abrasive" trace after conducting the experimental studies (the stage of the steady-state period of the wear process).

Table IV. Surface morphology in the area of the "abrasive" trace on the blade with the coating on the convex (a) and concave (b) sides

	Compressor blade without the coating	Compressor blade with the coating
Concave side	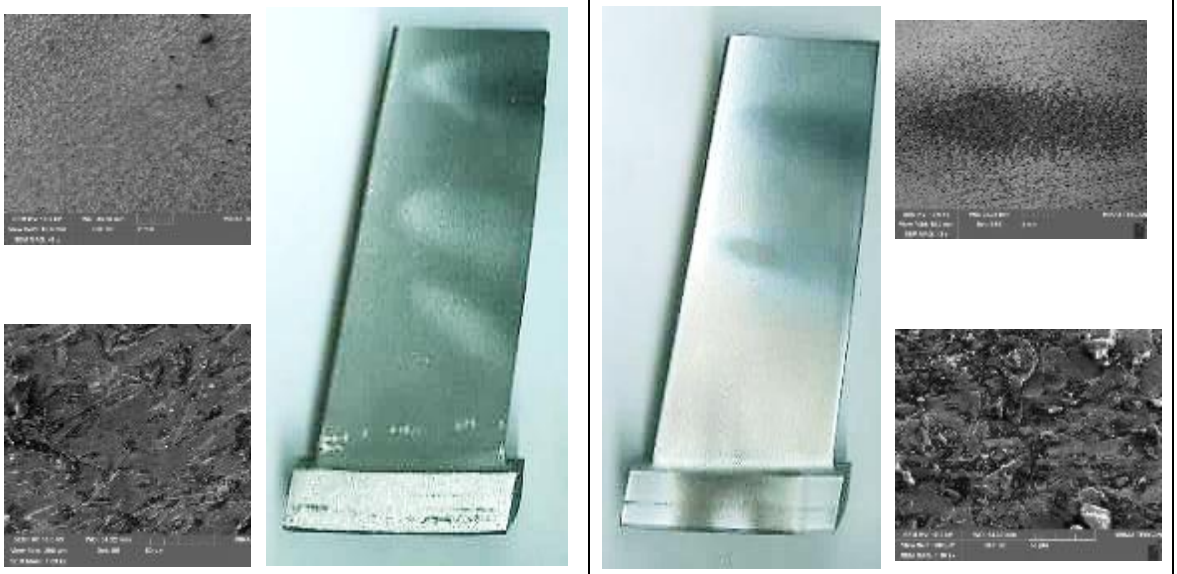	
Convex side		

It should be noted that the functional working surface of a blade has a complex geometric shape. Therefore, the pattern of wear on a curved surface may differ from a flat one. This is an important circumstance that turns out to be essential when describing the dynamics of solid particle erosion of real products. Based on the morphology of the surface of the obtained tracks, it follows that when interacting with the convex side of the two components, the impact of the air-abrasive flow – impact and cutting – shows the second component more significantly. In the case of interaction with the concave side of the blade, the impact component of the air-abrasive flow affects the intensity of wear more significantly. One part of the solid particles "slips" along the surface of the blade, while the other part gets stuck directly in the material itself. This observation, in our opinion, will affect the character of the solid particle erosion curve when the angle of attack of the flows changes in the direction different from the maximum value.

VIII. CONCLUSION

1. As a result, an ion-plasma coating based on Cr-CrC was formed using additive technologies on a part of the compressor blade. A complex of studies of its properties was also conducted, including those concerning resistance to solid particle erosion.

2. The steady-state speed of solid particle erosion on the convex and concave sides of the rotating blade without coating with an average angle of attack of the air-abrasive flow of 30 degrees is almost the same.

3. The proposed composition of the coating increases the resistance of the rotating blade to wear by solid particles by, on average, not less than two times.

4. The coating reveals its protective properties on both sides of the blade section. The use of the developed composition allows reducing twice the steady-state rate of wear of the base material on the concave side. On the convex side, the rate of wear of the material with and without the coating at an angle of attack of the air-abrasive flow of 30 degrees turned out to be equal.

IX. ACKNOWLEGMENT

The results of the work were obtained with the financial support of the Russian Science Foundation as part of the implementation of the Agreement No. 17-79-10460 dated July 28, 2017.

REFERENCES

1. D. Gu, Y.C Hagedorn, W. Meiners, G. Meng, B.R.J Santos, K. Wissenbach, et al, "Densification behavior, microstructure evolution, and wear performance of selective laser melting processed commercially pure titanium". *Acta Mater*, *vol.* 60, 2012, pp.849–60.
2. T.T. Wohlers, and T. Caffrey, "*Wohlers report 2015: 3D printing and additive manufacturing state of the industry annual worldwide progress report*". Fort Collins: Wohlers Associates, 2015.
3. B. Baufeld, V.D.O. Biest, and R. Gault. "Additive manufacturing of Ti–6Al–4V components by shaped metal deposition: microstructure and mechanical properties". *Mater Des*, *vol. 31*, 2010, pp. 106–11.
4. M. Schmidt, M. Merklein, D. Bourell, D. Dimitrov, T. Hausotte, K. Wegener, L. Overmeyer, F. Vollertsen, and G.N. Levy, "Laser based additive manufacturing in industry and academia". *CIRP Annals - Manufacturing Technology*, *vol. 66*, 2017, pp. 561–83.
5. W. Reschetnik, J.-P. Bruggemann, M.E. Aydinoz, O, Grydin, K.-P. Hoyer, G. Kullmer, and H.A. Richard, "Fatigue crack growth behavior and mechanical properties of additively processed EN AW-7075 aluminum alloy". The paper was presented on *The 21st European Conference on Fracture*, *ECF21*, 20-24 June 2016, Catania, Italy Procedia Structural Integrity, vol. 2, 2016, pp. 3040–8.
6. S. Leuders, M. Vollmer, F. Brenne, T. Stroster, T. and Niendorf, "Fatigue strength prediction for titanium alloy TiAl6V4 manufactured by selective laser melting". *Metallurgical and materials transactions*, *vol. 46A*, 2015, pp. 3816-23.
7. Y. Fang, X. Jiang, T. Song, D. Mo, and Z. Luo, "Pulsed laser welding of Ti-6Al-4V titanium alloy to AISI 316L stainless steel using Cu/Nb bilayer". *Materials Letters*, *vol. 244*, 2019, pp. 163–6.
8. Y. Sun, Y. Gong, Y. Liu, M. Cai, X. Ma, and P. Li, "Experimental investigation on effects of machining parameters on the performance of Ti-6Al-4V microrotary parts fabricated by LS-WEDT". *Archives of civil and mechanical engineering*, *vol. 18*, 2018, pp. 385–400.
9. M. Dharamendara, and N. Jegadeeswaran, "Development of Laser Heat Treatment HVOF Coating to Combat Oxidation on Gas Turbines". *Materials Today: Proceedings*, vol. 5, 2018, pp. 24937–43.
10. N.N. Cherenda, A.V. Basalaic, V.I. Shymanski, V.V. Uglov, V.M. Astashynskid, A.M. Kuzmitskid, A.P. Laskovneve, and G.E. Remnev, "Modification of Ti-6Al-4V alloy element and phase composition by compression plasma flows impact". *Surface & Coatings Technology*, *vol. 355*, 2018, pp. 148–54.
11. X. Zhao, G.H. Tang, Z. Liu, and Y.-W. Zhang, "Finite element analysis of anti-erosion characteristics of a material with patterned surface impacted by particles". *Powder Technology*, *vol. 342*, 2019, pp. 193–203.
12. RD 153-34.1-17.462-00. "*Guidelines on the procedure for assessing the performance of working blades of steam turbines in the process of manufacturing, operation and repair*".
13. H. Zhang, Z. Li, W. He, B. Liao, G. He, X. Cao, and Y. Li, "Damage evolution and mechanism of TiN/Ti multilayer coatings in sand erosion condition". *Surface & Coatings Technology*, *vol. 353*, 2018, pp. 210–20.
14. A.A. Siddiqui, A.K. Dubey, and C.P. Paul, "A study of metallurgy and erosion in laser surface alloying of AlxCu0.5FeNiTi high entropy alloy". *Surface & Coatings Technology*, *vol. 361*, 2019, pp. 27–34.
15. K.S. Selivanov, A.M. Smyslov, Y.M. Dyblenko, and I.P. Semenova, "Erosive wear behavior of Ti/Ti(V,Zr)N multilayered PVD coatings for Ti-6Al-4V alloy". *Wear*, *vol. 418–419*, 2019, pp. 160–6.
16. J. Y. Lek, A. Bhowmik, A. W.-Y. Tan, W. Sun, X. Song, W. Zhai, P. J. Buenconsejo, F. Li, E. Liu, Y. M. Lam, and C. B. Boothroy, "Understanding the microstructural evolution of cold sprayed Ti-6Al-4V coatings on Ti-6Al-4V substrates". *Applied Surface Science*, *vol. 459*, 2018, pp. 492–504.
17. J. Lin, R. Wei, F. Ge, Y. Li, X. Zhang, F. Huang, and M. Lei, "TiSiCN and TiAlVSiCN nanocomposite coatings deposited from Ti and Ti-6Al-4V targets". *Surface & Coatings Technology*, *vol. 336*, 2018, pp. 106–16.
18. Top 3D Shop. "*3D-printer Concept Laser M2 Cusing*" [online]. Available: https://top3dshop.ru/kupit-3d-printer/concept-laser-m2-cusing.html
19. K. Mouralova, J. Kovar, L. Klakurkova, P. Blazik, M. Kalivoda, and P. Kousal, "Analysis of surface and subsurface layers after WEDM for Ti-6Al-4V with heat treatment". *Measurement*, *vol. 116*, 2018, pp. 556–64.
20. J. Günther, S. Leuders, P. Koppa, T. Tröster, S. Henkel, H. Biermann, and T. Niendorf, "On the effect of internal channels and surface roughness on the high-cycle fatigue performance of Ti-6Al-4V processed by SLM". *Materials and Design*, *vol. 143*, 2018, pp. 1–11.
21. A.B Tkhabisimov, A.F Mednikov, A.Yu Marchenkov, O.S Zilovaand and A.A Burmistrov, "Metallographical researches results of titanium alloy Ti-6Al-4V samples obtained by using traditional and additive technologies". *Journal of Physics: Conference Series*, *vol. 1050*(1), 2018.
22. MPEI. "*Equipment*" [online]. Available: http://usu-erosion.mpei.ru/equipment/Pages/default.aspx
23. ASTM G76 – 13 Standard Test Method for Conducting Erosion Tests by Solid Particle Impingement Using Gas Jets.